Chief Editor
Dr. A. Singaraj, M.A., M.Phil., Ph.D.
Editor
Mrs.M.Josephin Immaculate Ruba

EDITORIAL ADVISORS

1. Prof. Dr.Said I.Shalaby, MD,Ph.D.
Professor & Vice President
Tropical Medicine,
Hepatology & Gastroenterology, NRC,
Academy of Scientific Research and Technology,
Cairo, Egypt.
2. Dr. Mussie T. Tessema,
Associate Professor,
Department of Business Administration,
Winona State University, MN,
United States of America,
3. Dr. Mengsteab Tesfayohannes,
Associate Professor,
Department of Management,
Sigmund Weis School of Business,
Susquehanna University,
Selinsgrove, PENN,
United States of America,
4. Dr. Ahmed Sebihi
Associate Professor
Islamic Culture and Social Sciences (ICSS),
Department of General Education (DGE),
Gulf Medical University (GMU),
UAE.
5. Dr. Anne Maduka,
Assistant Professor,
Department of Economics,
Anambra State University,
Igbariam Campus,
Nigeria.
6. Dr. D.K. Awasthi, M.SC., Ph.D.
Associate Professor
Department of Chemistry,
Sri J.N.P.G. College,
Charbagh, Lucknow,
Uttar Pradesh. India
7. Dr. Tirtharaj Bhoi, M.A, Ph.D,
Assistant Professor,
School of Social Science,
University of Jammu,
Jammu, Jammu & Kashmir, India.
8. Dr. Pradeep Kumar Choudhury,
Assistant Professor,
Institute for Studies in Industrial Development,
An ICSSR Research Institute,
New Delhi- 110070, India.
9. Dr. Gyanendra Awasthi, M.Sc., Ph.D., NET
Associate Professor & HOD
Department of Biochemistry,
Dolphin (PG) Institute of Biomedical & Natural Sciences,
Dehradun, Uttarakhand, India.
10. Dr. C. Satapathy,
Director,
Amity Humanity Foundation,
Amity Business School, Bhubaneswar,
Orissa, India.

ISSN (Online): 2455-7838
SJIF Impact Factor : 6.093

EPRA International Journal of

Research & Development (IJRD)

Monthly Peer Reviewed & Indexed
International Online Journal

Volume: 3, Issue:12, December 2018

Published By
EPRA Journals

CC License
BY NC ND

SJIF Impact Factor: 6.093 Volume: 3 | Issue: 12 | December | 2018 ISSN: 2455-7838(Online)
EPRA International Journal of Research and Development (IJRD)

A REVIEW ON CHARACTERIZATION OF VERSATILE DOUBLE-SIDED INCREMENTAL FORMING

Bhaskar R. S.
Department of Mechanical Engineering, IIMT Engineering College, Ganga Nagar, Meerut, UP, India

ABSTRACT

In modern era uses of Double Sided Incremental Forming (DSIF), we have discussed various characteristics forms of DSIF like Electrically assisted-DSIF, hybrid DSIF tool path strategy, mixed DSIF tool path strategy, Accumulative DSIF and DSIF with capabilities and challenges. DSIF is more advantageous over Single point Incremental forming (SPIF) on the basis of conduction, convection, radiation, combined electric heat and friction heat, tool path, working temperature surface finish, discharge phenomena and geometric accuracy on the Ti6Al4V material. A form of DSIF is latest die less forming process of incremental Sheet Metal forming (ISF) for improving surface finish, their geometric accuracy while reducing the forming time could be improved by using the enhanced technologies.

KEYWORDS: *DSIF, Ti6Al4V, Electric heating, Surface Finish, Geometric accuracy*

1. INTRODUCTION:

There are various industries including the aerospace, marine, automotive and biomedical industries, the use of titanium alloys is steadily increasing in many technological applications due to their high strength-to-weight ratio, elevated corrosion resistance and excellent biocompatibility [1]. Among the titanium alloys, Ti6Al4V is the most widely used. Titanium and Its alloy (Ti6Al4V) prove suitable for replacing and strengthening damaged bones. Ti6Al4V is the titanium alloy, otherwise known as a Grade 5 alloy or the 'iron fist' of the titanium industry because it is the most popular. It is light weight, strong and corrosion resistance. It is composed of 6% Aluminum, 4% Vanadium, 0.25% Iron, 0.2% Oxygen and 89.55% Titanium it is an all-round material that has multiple functions.

To increase the geometric accuracy of the basic form of ISF, i.e., of Single Point Incremental Forming (SPIF), where the sheet is locally deformed by one tool (Fig. 1a), different variants have been proposed, ranging from Multi Pass Incremental Forming, covering the entire [2] or partial [3] forming areas repeatability, to Double-Sided Incremental Forming (DSIF), in which a bottom tool, added on the opposite side of the sheet, peripherally moves along with the top tool from the sheet's outward to its inward position while shifting downward, as represented in Fig. 1b [4].

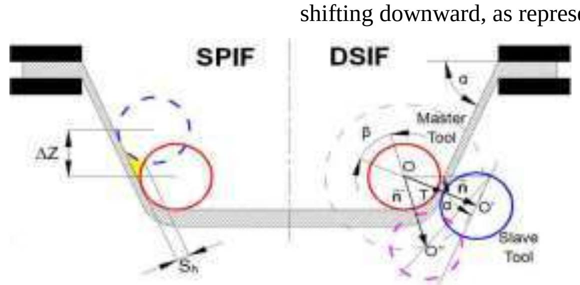

Fig. 1. Schematic representation of a) SPIF and b) DSIF.

All ISF techniques face the challenge of forming difficult-to-form materials [5], such as Ti6Al4V, for which an increase in forming temperature can overcome their limited formability at room temperature [6]. Among the different heating methods proposed in the literature, e.g., conduction, convection, radiation, friction and electricity [7], the Electrically-assisted Incremental Sheet Forming process (E-ISF) is the most flexible with a limited equipment cost [5]. Consequently, different hot ISF methods have been developed and these approaches are summarized as follows:

Convection: Various forming temperatures have been employed and the experiment results show that the forming limit increased as the forming temperature elevated. However, they also found that it was difficult to accurate control the forming temperature by adopting hot air blowers as the heat source.

Conduction: In this system, a heater band was mounted at the external surface of the fixture. Other than the local heating approach, this technology has to globally heat the whole sheet during the forming process, which reduces the energy efficiency.

Radiation: Duflou et al. [8] proposed a laser-assisted ISF process. In this process, a laser beam is employed to locally heat the sheet.

Friction heat: Otsu et al. [9] employed the frictional heat generated between the rotating tool and the static sheet to improve the material formability.

Electric heating: Fan et al. [10] proposed an electric hot incremental sheet forming (E-ISF) process.

Combined electric heat and friction heat:

In SPIF, only one forming tool is employed, which only has limited process capability in further improving the existing problems. In recent years, the DSIF based E-ISF process, namely the electrically-assisted double side incremental sheet forming (E-DSIF), has been proposed. Cao et al [11] firstly proposed the combination of electricity-assisted forming and DSIF process. Meier and Magnus [12] presented a robot-based E-DSIF process, which demonstrated the feasibility of E-DSIF. Asgar et al [13] employed the electric plus other than the direct current in the DSIF process and successfully fabricate the titanium alloys. Although the E-DSIF process shows great potential, there is limited investigation due to a series of challenges, such as the rough surface finish and inaccurate part geometry. In addition, slave tool and sheet may lose contact in the DSIF process [14, 15]. This becomes a seriously problem in E-DSIF as electric current cannot pass through the too-sheet interface when losing contact occurs.

2. E-DSIF PRINCIPLE AND MACHINE DESIGN

Based on the proposed concept, the E-DSIF machine has been developed shown in Fig. 2. This machine employed a 6-Axis PC-based control system from Power Automation to ensure the synchronized motion of master and slave tools. In addition, a direct current (DC) power supply with maximum current of 800A and voltage of 15V has been utilized to input specified energy to heat the materials. To reduce the tool oxidation, high temperature titanium alloy was employed as tool material. In addition, a thermal camera was employed to monitor the sheet temperature. To obtain the correct temperature value, the temperature range was set to correct values in the thermal camera software and thermocouple was employed to calibrate the thermal cameral. During the calibration process, the emissivity was adjusted to match the temperatures obtained in thermocouple and thermal cameral. In this way, the emissivity parameter can be determined and the thermal cameral can be calibrated before ISF experiments D. K. Xu et.al.[16].

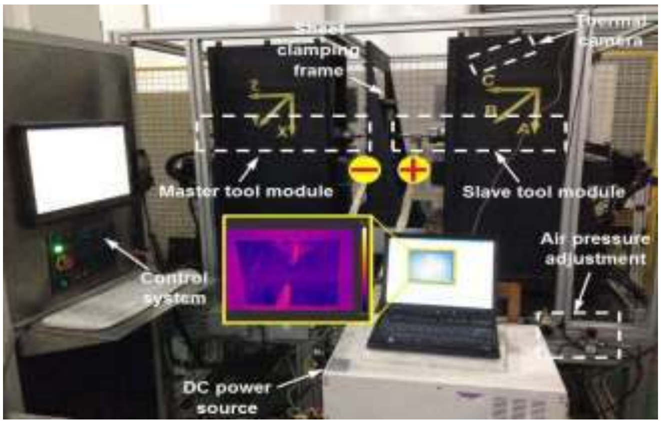

Fig. 2 Experimental setup of E-DSIF system

2.1 E-DSIF Tool path

In the current study of the SPIF process, the forming tool follows a continuously helical path to deform the sheets from outside towards inside. To major's parameters; incremental depth Z and scallop height S_h are employed to control the interval between adjacent helical paths as shown in Fig. 1. Compared to traditional contour tool path, the adopted helical tool path is able to avoid unexpected failure by eliminating the phenomenon of discharge in E-ISF, which also had been confirmed by Shi et al. [17]. Concerning the E-DSIF tool path, as two tools are involved, a series of point couples has to be generated to represent the positions of the both master tool and slave tool centers during the forming process. In this work, the master tool path that expressed by a series of point will be generated first. In the master tool path generation, contours have been generated base on the designed part by using the z-height slicing method. These contours have then interpolated to helical tool paths. The technical details can be referring to the Malhotra's tool path generation algorithm [18].

2.2 Tool path Parameters

The geometric accuracy of the formed parts was explored as a function of two key tool path parameters, namely, the incremental depth and relative position of the supporting tool. In DSIF, the squeeze factors Figure 3 Indicates the magnitudes of squeezing within the local area between the tools, while the surface normal is used to orient the tip of the supporting tool with respect to the forming tool, or the top tool. When s=1.0, the top tool and the bottom tool is just touching the sheet and when s<1.0, the top and the bottom tool are actively squeezing the sheet metal. Values of s =1.0, 0.9, 0.8, 0.75 were used in DSIF and in the D- stage of MDSIF to the study the effect of sheet squeezing on achievable geometric accuracy[1].

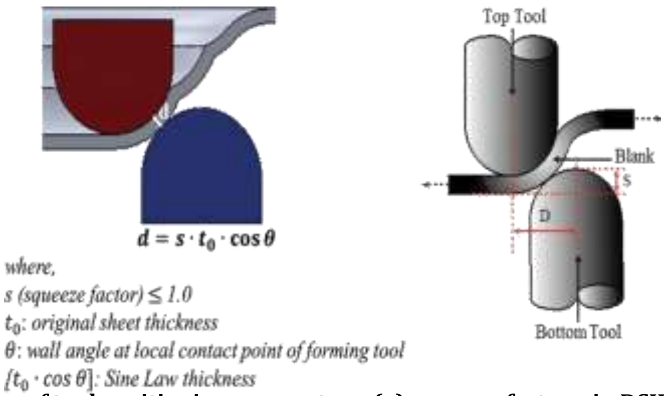

Fig.3. Definition of tool positioning parameters: (a) squeeze factor s in DSIF (b) s and d in ADSIF

3. CORRELATION BETWEEN THE E-DSIF FRACTURE SURFACES AND THE STRESS STATE

Based on the analytical model proposed by Lu et al. [19] for the DSIF process, the deformation area in E-DSIF can be split into three zones, as represented in Fig. 8a. Zone I is the portion of the sheet that first comes into contact with the top tool; Zone II is the one that is squeezed between the two tools; Zone III is related to the part of the material that has been already formed by the two tools, but is still in contact with only the top tool. Therefore, Zone I and Zone III are characterized by tensile stresses in the meridional direction, since the material is in contact only with the top tool, without any squeezing effect from the bottom tool [19], while Zone II is a compressive area because of the pressure applied by the bottom tool in the radial direction.

According to [19], the pressure in Zone II postpones fracture occurrence due to the Drop Of Stress Triaxiality (DOST) phenomenon, meaning that the fracture is not likely to initiate in this compressive area. Moreover, considering that in the E-DSIF process the tools-sheet contact area (Zone II) is heated through the Joule effect, which leads to an increase in the material's ductility as proven in [20], it is even less likely that fracture starts in Zone II. On this basis, it can be assumed that fracture starts in the area of the sheet that has been already formed (Zone III in Fig. 4a), which is characterized by a lower temperature and a reduced resistance section resulting from thinning in the radial direction. This is related to the negative strain in the radial direction that, considering volume conservation, results from the fact that convex shapes, such as the desired geometry in this study, lead to positive strain loading paths in the major (ε_1) vs. minor (ε_1) true strains space, as reported in [21]. Based on the stress state analysis, thinning is caused by the tensile stress operating in the meridional direction.

Zone III, which is in contact only with the top tool as in SPIF [22], beside the tensile stresses, is subjected also to bending around the tool, causing the material at the outer surface to stretch more as compared to the material at the inner surface, thus resulting in a higher plastic strain on the outer surface. In the same zone, friction at the tool-sheet contact along the meridional and circumferential directions results in $\boldsymbol{\tau_{r\Theta}}$ and $\boldsymbol{\tau_{r\theta}}$ tangential stresses, respectively, as represented in Fig. 4b, the latter being more significant because the tool moves mainly in the circumferential direction [19].

Summarizing all the aforementioned aspects, it can be stated that fracture in E-DSIF occurs by progressive thinning of the sheet under tension, starting from the outer surface. Consequently, considering the conventional classification of fracture modes [23], fracture in E-DSIF can be classified as Mode I, or tearing. To note that tearing is considered as a conventional fracture mode also in SPIF [21, 24].

A further proof of fracture by tearing in E-DSIF is given by the orientation of the dimples. Indeed, as the dimples in the tearing fracture surfaces point towards the origin of fracture [23], the dimples in the E-DSIF fracture surfaces are orientated towards the outer side; this was demonstrated to be the starting point of fracture because of its higher damage.

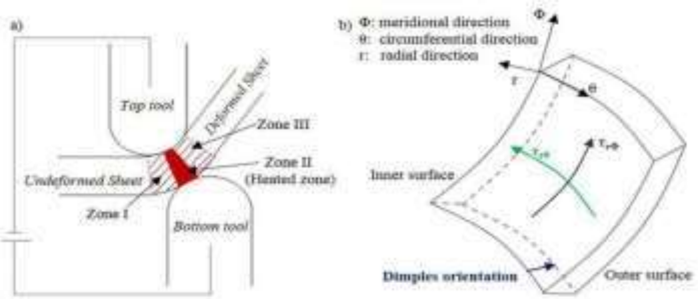

Fig. 4. a) Deformation zones in the E-DSIF process; b) shear stress components in a small element through the thickness and detail of the dimple orientation.

4. 1 The material and working temperature in the E-DSIF process:

As both E-SPIF and E-DSIF are localized heating processes, the location of maximum sheet temperature changes in correspondence with the movement of the heat source. The typical temperature variation history for both E-SPIF and E-DSIF process is illustrated as shown in Fig.5 As can be seen in the Figure, similar trends of temperature variation can be observed for the two processes. The maximum temperature gradually increases from room temperature to the target forming temperature of 200 °C in about 200s. After that the maximum temperature is maintained within the target range of 200±10 °C by manually adjusting the input current. Concerning the temperature distribution as shown in the top left corner, it can be observed that the temperature distribution is non-uniform, and the maximum temperature appears at the location where the forming tool contacts with the sheet. Considering the temperature variation at specific point, cyclic heat loading is observed as the monitored temperature oscillates at the specific location. When the tool approaches the region where the specific point locates, the temperature at the point periodically reaches its maximum value in every pass. When the tool moves away to a next location after the temperature achieves its peak value of about 210 °C, the minimum temperature in the cycle can drop down to about 80 °C. This measurement suggests the unlike the single cycle of temperature raising and dropping in conventional hot stamping, cyclic temperature change exists in the E-ISF process due to its localized heating nature. In addition, this cyclic heat impact may results a different microstructure revolution in the forming process. As temperature rising up and drop down in very short period of time, there may not be sufficient time for recrystallization.

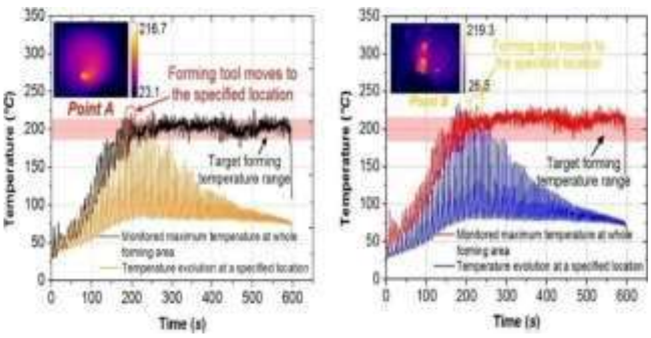

Fig. 5 Monitored temperature of the sheet during forming process: (a) E-SPIF; (b) E-DSIF

4.2 Tool head designs and surface finish measurement

Arithmetic average of the 3D roughness S_a in Eq. (1) was calculated to quantitatively describe the surface finish.

$$S_a = \frac{1}{A}\iint_A |Z(x,y)| dxdy \text{.....................}(1)$$

Where A is the area of measured region, $Z(x,y)$ denotes the values of peaks and valleys on the region. Using the microscope and the described measurement approach, the surface topography in initial sheet is given in Fig. 6. As can be seen in the figure, the initial S_a value of the original sheet surface is 0.721μm, which indicates very good surface finish. This value is employed as a reference for the comparison between the formed parts in the following sections.

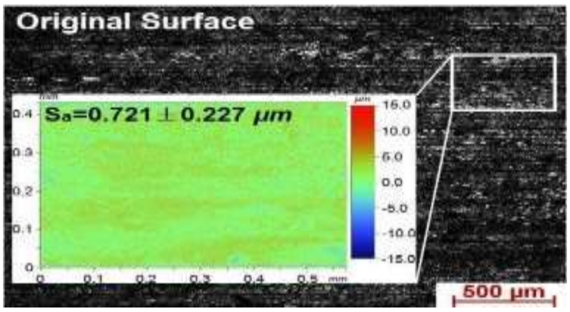

Fig. 6 Surface finish of original sheets

4.3 Investigation of surface finish in E-SPIF and E-DISF

Using the described approaches, the surface topography of E-SPIF and E-DSIF processes are compared as shown in Fig. 7 and 8.

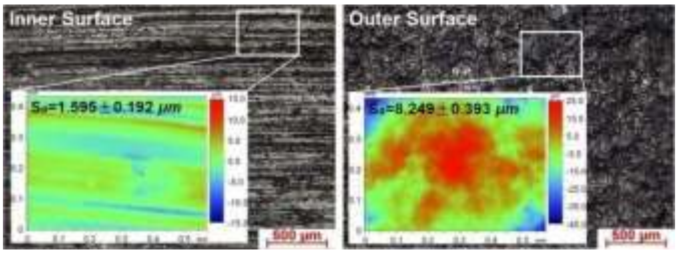

Fig. 7 Surface finish of components formed in E-SPIF with rigid tool: (a) inner surface and (b) outer surface

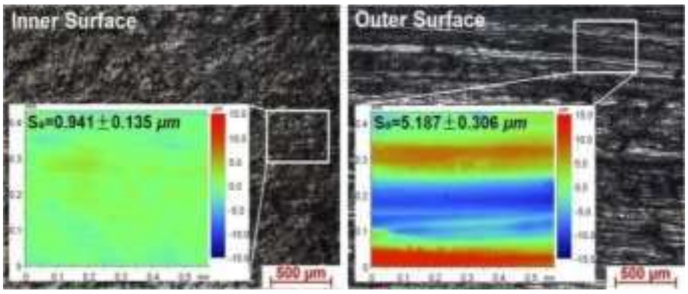

Fig. 8 Surface finish of components formed in E-DSIF with two roller-ball tools: (a) inner surface and (b) outer surface

4.4 Elimination of discharge phenomenon

The above experimental results of surface finish suggest that employing the rigid tool as slave tool in the E-DSIF process has obvious advantages since the roller-ball tool may cause electric discharge. In those cases, to maintain the temperature of sheet at a certain level, current continuously passes into the sheet deformation area through the slave tool. As a result, regardless of what type of tool is used, the accumulated heat continuously raises the temperature of slave tool. This is confirmed by the monitored temperature of the slave tool as shown in Fig. 9, in which the temperature of slave tool continues to increase during the entire forming process. Therefore, the friction condition may be worsened when the temperature of forming tool is even higher than the sheet. In addition, the above result also suggests that although the rigid tool with sliding friction condition is employed, it will not cause the surface damage. This is because the slave tool does not take the major forming load and the corresponding contact pressure is much lower comparing to master tool.

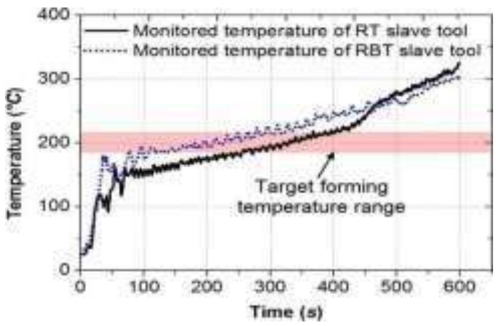

Fig. 9 The slave tool temperature during E-DSIF process (RT-Rigid tool and RBT-Roller-ball tool)

4.5 The E-DSIF geometrical accuracy

In E-SPIF and E-DSIF the geometry of the formed components in E-SPIF and E-DSIF were compared to the nominal shape as shown in Fig. 15. It can be observed that before the components reached the depth of around 7.5 mm, the produced shapes matched well with the desired shape in both cases. However, after this depth, a significant geometrical deviation can be observed due to the bending effect at the initial forming stage. As compared with E-SPIF, the maximum geometrical deviation in E-DSIF is reduced by 29.8 %, from 3.2 mm to 2.2 mm. This reduction mainly attributes to the support from the slave tool at outer surface. Although E-DSIF shows an enhanced capability on geometrical accuracy, the deviation is still considerable large.

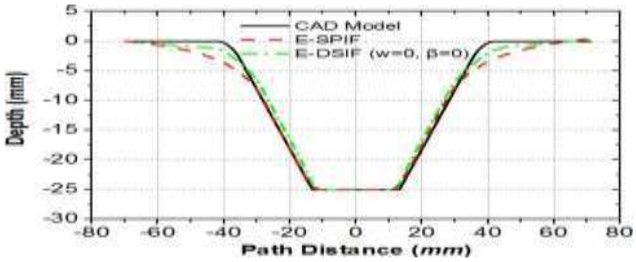

Fig. 10 Comparison of geometrical accuracy in E-SPIF and E-DSIF

4.6 A DSIF, hybrid DSIF and ADSIF tool path strategy

The result obtained in Fig. 11 suggests that the main shape deviation comes from the bending of sheet in the fillet area at the initial forming stage. This inaccuracy cannot be minimized by optimizing the forming parameters. Alternatively, direct modification of tool path may have larger impact on the geometric accuracy. In this work, a hybrid DSIF tool path strategy has been proposed as illustrated in Fig. 11. At the initial stage, the slave tool acts similarly as the role of a backing plate in SPIF process. Only the master tool will move downward while the slave tool will remain at the same level in Z direction. In this way, the fillet can be formed with minimized bending effect and the corresponding shape deviation will be reduced. After forming the fillet, the two tools will move down simultaneously as those in conventional DSIF process. Using this strategy, the geometrical deviation caused by the bending effect may be reduced while the advantages of DSIF such as squeezing effect can still be maintained.

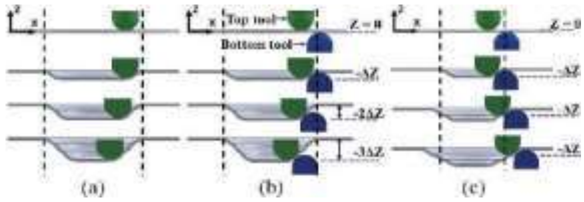

Fig. 11 Toolpath strategies in incremental forming: (a) SPIF (b) DSIF and (c) ADSIF

The profile measurement in Fig. 12 confirmed that a more accurate geometry can be obtained by using the proposed hybrid DSIF tool path strategy as compared to the one formed by using conventional DSIF tool path strategy. The maximum shape deviation decreased by 30.16%, from 2.2 mm to 1.5 mm. In addition, it can also be observed that the maximum shape deviation did not occur at the region of side wall, but transferred to the flat surface of the formed component. A region with bulges was detected as shown in the figure. This phenomenon attributes to the higher backing pressure imposed onto the sheet by the slave tool during forming the fillet. The solution was to reduce the backing pressure as 0MPa in the forming of fillet, and then increase to the

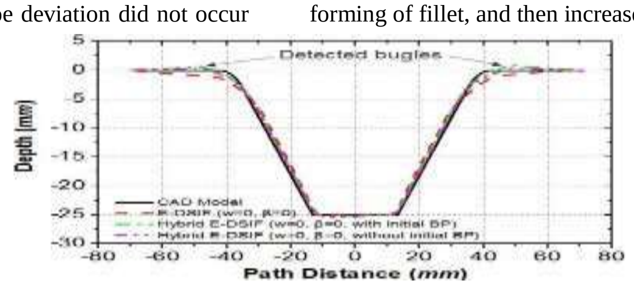

Fig. 12 Improved geometrical accuracy by using hybrid DSIF tool path strategy

value in forming the inclined wall. Through this adjustment the bugle height reduced from 1.6 mm to 0.4 mm. The maximum geometrical inaccuracy at the side wall was 1.4 mm which was only 60.9% of the value obtained by using the conventional tool path strategy.

4.7 Geometric error quantification

The final geometric error (δ_{final}) may be considered as a sum of shape deviations generated in forming, unclamping and trimming, which can be expressed as:

$$\delta_{final} = \delta_c + \delta_{uc} + \delta_t \text{.................}(2)$$

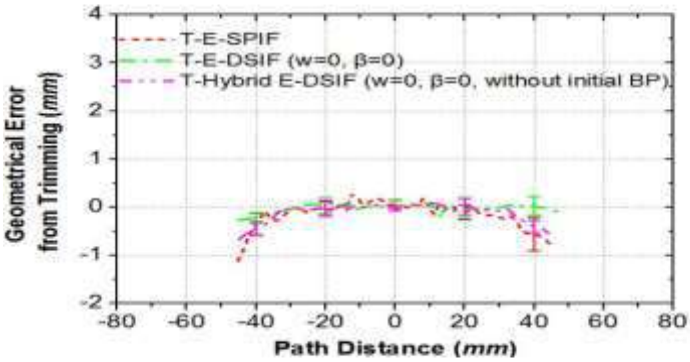

(a)

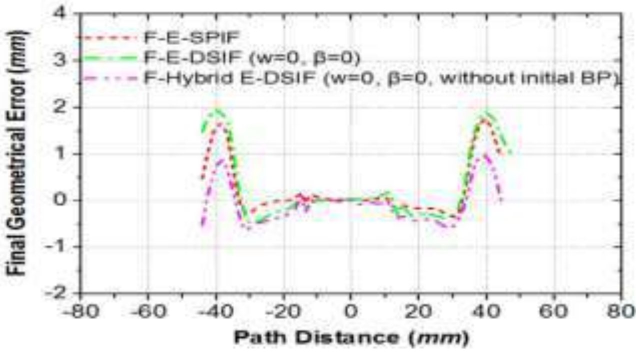

b)

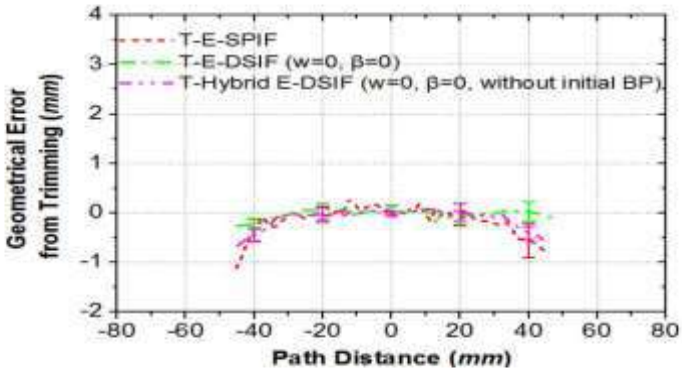

C

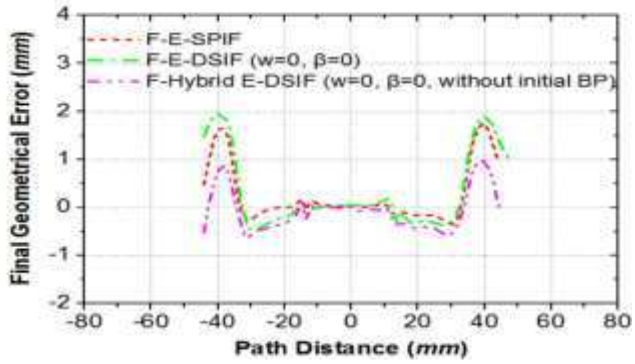

d

Fig. 13 Decomposition of shape deviation: (a) δc *(*b) *δuc (*c) *δt* and (d) *δfinal*

Where $\boldsymbol{\delta_c}$ is the error measured when the formed components were still clamped on the frame, $\boldsymbol{\delta_{uc}}$ and $\boldsymbol{\delta_t}$ are the geometrical errors obtained from unclamping and trimming, respectively. Using the measured profiles in Fig. 13, the geometric errors of $\boldsymbol{\delta_c}$, $\boldsymbol{\delta_{uc}}$ and δ_t in each step can be obtained, as shown in Fig. 13.

4.8 Geometric Accuracy:

The ADSIF is able to offer a performed shape that is closer to the desired geometry than DSIF. DSIF, where the tools move along the desired geometry rather than staying in plane as in ADSIF is capable of turning the performed shape. The combination of the two tool path strategies in MDSIF is able to improve the geometric accuracy [25].

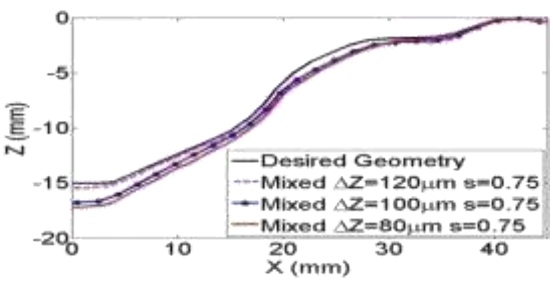

Fig 14.Geometrics formed with squeeze factor s=0.75 with various incremental depths

5. RESULT AND DISCUSSION

5.1 The E-DSIF process

Comparing to the conventional E-SPIF process, the two-tool approach in the E-DSIF process has some advantages: the backing plate becomes unnecessary and the spring back turns out to be smaller due to a different sheet deformation mode. Comparing to other heating methods such as laser assisted incremental forming, the equipment cost is much lower and the sheet can be heated at the same time as deformation without complex optical system. However, the E-DSIF method may be more suitable for materials with larger electrical resistance. Although material such as aluminum alloys can also be formed by using this approach, larger electrical current is required to heat up the sheet which is not energy efficient.

5.2 The E-DSIF Surface finish

This will increase the process complexity and pretreatment on sheet has to be performed before forming. Non-contact heating method such as laser may partly reduce this problem as the tool can be stay cooled to reduce the adhesion of material. For the E-ISF process, the electric current will pass and heat the tool. To overcome this problem, different forming tools and strategies have been employed to look for a solution. It was found that although the utilization of roller-ball tool is usually considered as a feasible way to improve the surface finish in ISF process, this research concludes that it cannot serve as an electrode because of the electric discharge due to unsteady contact

5.3 The E-DSIF Geometrical accuracy

Concerning the geometrical accuracy, the E-DSIF process provides greater possibilities in enhancing geometrical accuracy than the E-SPIF process. As the relative position between the master and slave forming tools can be varied, it offers higher degrees of flexibility in sheet deformation. In this work, the slave tool travels only in the horizontal direction without the downward movement and acts as a moving backing plate to suppress the geometrical deviation resulted from bending. After the forming of fillet, both forming tools will move down simultaneously as those in conventional DSIF process. In this way, the hybrid tool path not only reduces the bending effect, but also takes the advantages of DSIF.

Another interesting finding is from the different spring back behaviors between E-DSIF and E-SPIF strategies. As observed in Fig. 14, larger spring back can be observed for the E-SPIF part during unclamping and trimming process while those of the E-DSIF part is much smaller. Considering that all the parts have similar shape and stiffness, the varied spring back may imply different residual stresses resulted in the E-SPIF and E-DSIF processes: both E-DSIF processes may result in smaller residual stress than the E-SPIF process, which lead to the smaller spring back. This reduced residual stress may be caused by the additional material deformation due to tool squeezing. However, further study on direct measuring the residual stress may be necessary to confirm this point. The reduced spring back may also benefit the improvement of geometrical accuracy: if the spring back is smaller, it will be much easier to compensate that geometric error by modifying the tool path to reach higher accuracy.

DSIF is a cost effective process to form customized low volume products. However the following aspects need to be studied thoroughly to exploit DSIF capabilities. Compensation for multi stage strategy, Process design for achieving required mechanical and metallurgical properties, Reduce computational resources required prediction, Post processing treatment for enhancing the properties [26].

6. CONCLUSIONS

In this paper has tried to show versatile characteristics of DSIF approach with improving part surface and geometric accuracy. The Characteristics of Ti6Al4V in E-DSIF used to produce parts characteretised by double curvature convex shape and identifies the fracture mode. E-DSIF is more advantageous better surface finish, to reduce geometrical deviation and design of E-DSIF aimed at increasing formability and proper contact support tool achieved using force control can be avoided. E-DSIF reduces the spring back of finished parts during unclamping and trimming stages. Hybrid DSIF tool path strategy has been developed to further enhance geometric accuracy while reducing the forming time. Hybrid DSIF tool path strategies is to eliminate the geometrical deviation due to bending. Future will take machine compliance and tool deflection into account and develop more generalized DSIF parameters additional studies on the understanding of the ADSIF process are progress. ADSIF require the use of a very small incremental depth in order to form an accurate geometry which results in significantly increased forming time. However scaling up the process to form large components with good accuracy, forming complex geometries and studying in the mechanical and metallurgical properties are the gaps that need to be addressed to take DSIF into industrial use. The contact area between the two tools is heated through the Joule effect, thus will increase the material's ductility. In future application Ti6Al4V material to most widely use in many Industries aerospace, marine, biomedical and automobile structures (light weight, elevated corrosion resistance and excellent biocompatibility) in making advanced armour and weapons (due to strength) to make a eternal wire, used in a heart bypass, as an alternative to Nickel, which many are allergic to.

REFERENCES

1. *Beatrice Valoppi, Zixuan Zhang, Muyang Deng, Andrea Ghiotti, Stefania Bruschi, Kornel F. Ehmann, Jian Cao, "On the fracture characterization in Double-Sided Incremental Forming of Ti6Al4V Sheets at Elevated Temperatures", Elsevier B.V. July 2017, 407-416.*
2. *J. R. Duflou, J. Verbert, B. Belkassem, J. Gu, H. Sol, C. Henrard, A. M. Habraken, Process window enhancement for single point incremental forming through multi-step toolpaths. CIRP Annals - Manufacturing Technology 57/1 (2008) 253–256.*
3. *R. Malhotra, A. Bhattacharya, A. Kumar, N. V. Reddy, J. Cao, A new methodology for multi-pass single point incremental forming with mixed toolpaths. CIRP Annals - Manufuring Technology 60/1 (2011) 323–326.*
4. *B. Valoppi, A. Ghiotti, S. Bruschi, Elevated temperature behaviour of Ti6Al4V sheets with thermo-electro-chemical modified surfaces for biomedical applications. Proc. Inst. Mech. Eng. Part L J. Mater. Des. Appl., 2015.*
5. *JZ. Zhang, H. Ren, R. Xu, N. Moser, J. Smith, E. Ndip-Agbor, R. Malhotra, Z. Cedric Xia, K. F. Ehmann, J. Cao, A Mixed Double-Sided Incremental Forming Toolpath Strategy for Improved Geometric Accuracy. Journal of*

Manufacturing Science and Engineering 137/5 (2015) 51007.

6. *D. K. Xu, B. Lu, T. T. Cao, H. Zhang, J. Chen, H. Long, and J. Cao, "Enhancement of process capabilities in electrically-assisted double sided incremental forming," Mater. Des., vol. 92, pp. 268–280, 2015.*
7. *F. K. Chen, K. H. Chiu, Stamping formability of pure titanium sheets. Journal of Materials Processing Technology 170/1–2 (2005) 181–186. [14]. Ambrogio, L. Filice, G. L. Manco, Warm incremental forming of magnesium alloy AZ31. CIRP Annals - Manufuring Technology 57/1 (2008) 257–260.*
8. *Duflou JR, Callebaut B, Verbert J, De Baerdemaeker H. Laser Assisted Incremental Forming: Formability and Accuracy Improvement. CIRP Annals - Manufacturing Technology. 2007; 56:273-6.*
9. *Otsu M, Matsuo H, Matsuda M, Takashima K. Friction stir incremental forming of aluminum alloy sheets. Steel Research International. 2010; 81:942-5.*
10. *Fan G, Gao L, Hussain G, Wu Z. Electric hot incremental forming: A novel technique. International Journal of Machine Tools and Manufacture. 2008; 48:1688-92.*
11. *Cao J, Roth JT, Xia C, Gutowski T. A Hybrid Forming System: Electrical-Assisted Double Side Incremental Forming (EADSIF) Process for Enhanced Formability and Geometrical Flexibility. Report to DOE/EERE - Industrial Technologies Program, 8pp, October 2010. 2010.*
12. *Meier H, Magnus C. Incremental Sheet Metal Forming with Direct Resistance Heating Using Two Moving Tools. Key Engineering Materials. 2013; 554-557:1362-7.*
13. *Asgar J, Lingam R, Reddy NV. Tool path influence on electric pulse aided deformation during incremental sheet metal forming The 9th International Conference and Workshop on Numerical Simulation of 3D Sheet Metal Forming Prcesses. Melbourne, Australia2014. p. 840-3.*
14. *Malhotra R, Cao J, Beltran M, Xu D, Magargee J, Kiridena V, et al. Accumulative-DSIF strategy for enhancing process capabilities in incremental forming. CIRP Annals - Manufacturing Technology. 2012; 61:251-4.*
15. *Malhotra R, Cao J, Ren F, Kiridena V, Cedric Xia Z, Reddy NV. Improvement of Geometric Accuracy in Incremental Forming by Using a Squeezing Toolpath Strategy With Two Forming Tools. Journal of Manufacturing Science and Engineering. 2011; 133:061019.*
16. *D.K. Xu, B. Lu, T.T. Cao, H. Zhang, J. Chen, H. Long, J. Cao, Enhancement of Process Capabilities in Electrically-assisted Double Sided Incremental Forming. Materials and Design, 92. pp. (2016) 268-280.*
17. *Shi X, Gao L, Khalatbari H, Xu Y, Wang H, Jin L. Electric hot incremental forming of low carbon steel sheet: accuracy improvement. The International Journal of Advanced Manufacturing Technology. 2013; 68:241-7.*
18. *Malhotra R, Bhattacharya A, Kumar A, Reddy NV, Cao J. A new methodology for multi-pass single point incremental forming with mixed toolpaths. CIRP Annals - Manufacturing Technology. 2011; 60:323-6.*
19. *B. Lu, Y. Fang, D. K. Xu, J. Chen, S. Ai, H. Long, H. Ou, J. Cao, Investigation of material deformation mechanism in double side incremental sheet forming. International Journal of Machine Tools and Manufacture 93 (2015) 37–48.*
20. *B. Valoppi, S. Bruschi, A. Ghiotti, Modelling of Fracture Onset in Ti6Al4V Sheets Deformed at Elevated Temperature. Procedia Manufacturing 5 (2016) 248–258.*
21. *J. M. C. Soeiro, C. M. A. Silva, M. B. Silva, P. A. F. Martins, Revisiting the formability limits by fracture in sheet metal forming. Journal of Materials Processing Technology 217 (2015) 184–192.*
22. *R. Malhotra, L. Xue, T. Belytschko, J. Cao, Mechanics of fracture in single point incremental forming. Journal of Materials Processing Technology 212/7 (2012) 1573–1590.*
23. *Fractography, vol. 12. The Materials Information Company. ASM International (2001).*
24. *T. Madeira, C. M. A. Silva, M. B. Silva, P. A. F. Martins, Failure in single point incremental forming. International Journal of Advanced Manufacturing Technology 80/9 (2015) 1471–1479.*
25. *Zhang Z., Ren H., Xu R, Moser N., Smith J., Agbor E.N., Malhotra R., Zia Z. C. Ehman K. F., Jian C., " A Mixed Double Sided Incremental Forming Tool path Strategy for improved Geometric Accuracy", International Journal of Advanced Manufacturing Science and Engineering, V. 137, (2015), 051007-1-7.*
26. *N.V. Reddy, R Lingam, "Double Sided Incremental Forming: Capability and Challenges", IOP Conference series:1063 (2018)012170*